J. Synchrotron Rad. (1998). **5**, 1099–1101

X-ray contact microscopy system for spectromicroscopy of biological specimens

Atsushi Ito,[a]* Kunio Shinohara,[b] Yutaka Mizukami,[c] Hisako Nakano,[d] Keiji Yada,[e] Takayuki Uehara[c] and Toshio Honda[c]

[a]Department of Nuclear Engineering, School of Engineering, Tokai University, 1117 Kitakaname, Hiratsuka-shi, Kanagawa 259-12, Japan, [b]Radiation Research Institute, Faculty of Medicine, The University of Tokyo, 7-3-1 Hongo, Bunkyo-ku, Tokyo 113, Japan, [c]Department of Image Science, Faculty of Engineering, Chiba University, 1-33 Yayoi-cho, Inage-ku, Chiba-shi, Chiba 263, Japan, [d]Department of Radiation Research, Tokyo Metropolitan Institute of Medical Science, 3-18-22 Honkomagome, Bunkyo-ku, Tokyo 113, Japan, and [e]Aomori Public College, 153-4 Yamazaki, Goshizawa, Aomori 030, Japan. E-mail: aeito@keyaki.cc.u-tokai.ac.jp

(*Received 4 August 1997; accepted 8 December 1997*)

An X-ray contact microscopy system has been developed for the study of molecular and elemental distributions in biological specimens based on X-ray absorption characteristics. The system consists of a chamber for measuring XANES (X-ray absorption near-edge structure) of biomolecules, and a contact microscopy system for dried specimens with an electronic zooming tube. With this system the elemental distribution of carbon, nitrogen, oxygen, Ca and Fe in an HeLa cell has been studied, and the DNA-related image using a peak from the XANES profile of the DNA at the *K*-absorption edge of phosphorus has been obtained.

Keywords: spectromicroscopy; XANES; element analysis; mammalian cells.

1. Introduction

One of the most specialized applications of X-ray microscopy will be the mapping of elements and molecules in a biological cell using their specific absorption characteristics in the soft X-ray region. Spectromicroscopy utilizing XANES peaks at the *L*-absorption edge of calcium has been attempted for biological specimens containing Ca; for example, Kenny *et al.* (1985) first imaged calcium in human skull bone. Later, Buckley *et al.* (1993) imaged fine Ca phosphate deposits in a region of chondrocyte in femoral head sections. They discussed quantitative aspects of image formation using the XANES profile of Ca foil (Buckley *et al.*, 1994; Buckley, 1995). Imaging with a difference in chemical states of Ca has been performed by Buckley *et al.* (1994) for different distributions of Ca hydroxy apatite in bone and tricalcium phosphate in prostheses. Buckley *et al.* (1995) also compared XANES profiles of some Ca salts associated with osteoarthritis. Ade *et al.* (1992), followed by Zhang *et al.* (1994), applied XANES peaks at the *K*-edge of carbon to the molecular mapping of DNA in a chromosome using a difference in the spectrum of the C=C bond in DNA from that in bovine serum albumin. With a contact microscopy system in combination with an electronic zooming tube as a detector, we have obtained absorption spectra of intracellular regions of an HeLa cell over a wide wavelength range covering the absorption edges of major elements in biological specimens (Shinohara *et al.*, 1994; Ito *et al.*, 1996), and also attempted DNA imaging in a cell using an XANES peak at the *K*-edge of phosphorus (Shinohara *et al.*, 1997).

In the present study, we expanded our system to incorporate a chamber for the measurement of XANES profiles of isolated biological molecules, which enabled us to obtain a more accurate determination of XANES peaks prior to the imaging of the molecule. Furthermore, a computer program for the analysis of elements in a cell has been newly developed and provided improved images.

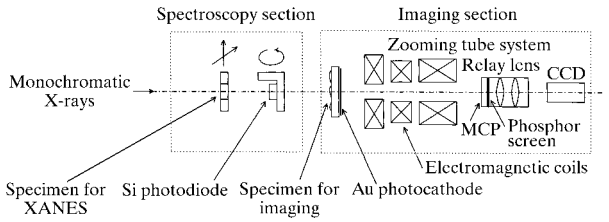

Figure 1
Layout of the X-ray contact microscopy system consisting of a spectroscopy section, and contact microscopy with an electronic zooming tube (an imaging section).

2. Materials and methods

2.1. *Experimental layout*

Fig. 1 shows the optical layout of an X-ray contact microscopy system. The system consists of two tandem-aligned parts for spectroscopy of thin films of biological specimens followed by contact microscopy of dried specimens. Monochromatic X-rays were obtained from BL-12A covering the *K*-edges of carbon, nitrogen and oxygen, and the *L*-edges of iron and calcium, and from BL-11B covering the *K*-edges of phosphorus and sulfur, at the Photon Factory, Institute of Materials Structure Science in Tsukuba, Japan. The energy resolution ($E/\Delta E$) was about 100 for BL-12A and 1500–2500 for BL-11B. After determining the energies of resonance peaks in XANES of biomolecules with a silicon photodiode detector (AXUV-100, International Radiation Detectors Inc., USA), the specimen and the detector were removed from the light path. Then, dried biological specimens can be imaged at the same wavelength and in the same light path.

2.2. *XANES measurements*

DNA from a calf thymus (Sigma Chemical Co., USA) and cysteine (Wako Pure Chemical Industries Ltd, Japan) in a dry thin film were prepared on a collodion film supported by an EM-grid. XANES profiles were measured at the *K*-edges of phosphorus and sulfur.

2.3. *Contact imaging*

Contact microscopy using an electronic zooming tube arranged in a user-friendly system for handling specimens has been described elsewhere (Shinohara *et al.*, 1997; Ito *et al.*, 1997). Human HeLa cells cultured on an SiN membrane were fixed with glutaraldehyde, and then dried. For the observation of mitotic cells, the cell division cycle was stopped by an 8 h treatment with 0.25 μg ml^{-1} nocodazole solution.

2.4. *Elemental analysis*

To obtain the intracellular distributions of the major elements, C, N, O, Ca and Fe, images were taken at both sides of the absorption edge of each element. The wavelengths were adopted so that they were situated beyond the region of XANES and are listed by Henke *et al.* (1993), who tabulated the optical data of elements. The transmittance (I/I_0) of an image in each pixel was obtained by dividing the photon intensity (I) in each pixel by I_0, the average for the area outside the cells. The following is the relation between optical density denoted as A_j ($= \log I_0/I$) and the content (mass thickness) of element i expressed as $\rho_i x$, where ρ_i and x are the density and the specimen thickness, respectively,

$$A_j \equiv -\log T(\lambda_j) = \sum_{i=1}^{n} \mu_i(\lambda_j)\rho_i x. \qquad (1)$$

In the equation, λ_j and n denote the wavelength and the number of elements, respectively: $T(\lambda_j)$ and $\mu_i(\lambda_j)$ represent the transmittance and the mass absorption coefficient of element i at wavelength λ_j, respectively. $\rho_i x$ can be obtained by subtracting A_j from $A_{j'}$ at both sides (λ_j and $\lambda_{j'}$) of the absorption edge of element i, under the approximation that mass absorption coefficients, μ, of elements other than i are equal at both wavelengths. However, this assumption would not be valid when λ_j and $\lambda_{j'}$ are not close. In our previous paper (Shinohara *et al.*, 1994), the carbon content (nitrogen and oxygen in some cases) was considered to be corrected for the mapping of other elements. Application of the least-squares method would be a better method particularly for mapping elements of minor fraction such as Ca and Fe. To obtain the minimum of $\sum_{j=1}^{m}(A_j^* - A_j)^2$, where m is the number of wavelengths and A_j^* is an experimental value, the following normal equation should be solved,

$$\begin{cases} \mu_{11}\rho_1 x + \mu_{12}\rho_2 x + \mu_{13}\rho_3 x + \ldots + \mu_{1n}\rho_n x = B_1 \\ \mu_{21}\rho_1 x + \mu_{22}\rho_2 x + \mu_{23}\rho_3 x + \ldots + \mu_{2n}\rho_n x = B_2 \\ \ldots \\ \ldots \\ \mu_{n1}\rho_1 x + \mu_{n2}\rho_2 x + \mu_{n3}\rho_3 x + \ldots + \mu_{nn}\rho_n x = B_n \end{cases} \qquad (2)$$

where

$$\mu_{pq} = \sum_{j=1}^{m} \mu_p(\lambda_j)\mu_q(\lambda_j) \qquad (p, q = 1 \rightarrow n),$$

$$B_p = \sum_{j=1}^{m} \mu_p(\lambda_j)A_j \qquad (p, q = 1 \rightarrow n).$$

The computer program for these procedures has been developed.

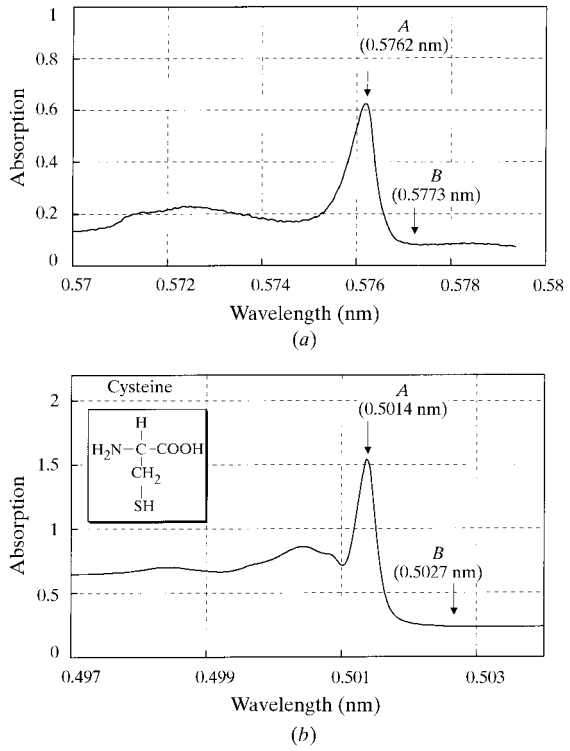

Figure 2
XANES profiles of (*a*) DNA at the *K*-edge of phosphorus, and (*b*) cysteine at the *K*-edge of sulfur.

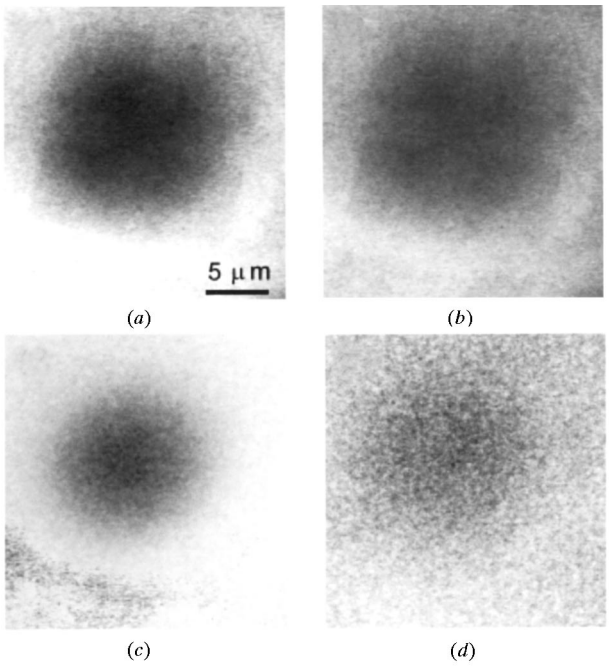

Figure 3
Ratio images of DNA- and cysteine-related molecules in a mitotic HeLa cell. (*a*) Image at *A* in the panel (*a*) of Fig. 2; (*b*) image at *B* in the panel (*a*) of Fig. 2; (*c*) ratio image of (*a*) and (*b*); (*d*) ratio image of cysteine-related molecules using the XANES profile of Fig. 2(*b*).

2.5. *Molecular distribution*

The molecular distribution in a biological cell was shown by the ratio image between the image at the peak wavelength of XANES of the molecule and that below the peak.

3. Results and discussion

3.1. *Molecular imaging of DNA-related P and protein-related S in a mitotic HeLa cell*

In Fig. 2(*a*) the prominent resonance peak of DNA was observed at the *K*-edge of phosphorus. Cysteine also has a large resonance peak at the *K*-edge of sulfur (Fig. 2*b*). The ratio image between the image at the peak (Fig. 3*a*) and that below the peak (Fig. 3*b*) of the XANES profile of DNA is shown in Fig. 3(*c*). Some structure of the DNA-related molecules in the central part of the cell was clear, which was in contrast with the sulfur image shown in Fig. 3(*d*). Identification of chromosomal structure would need further resolution and sensitivity.

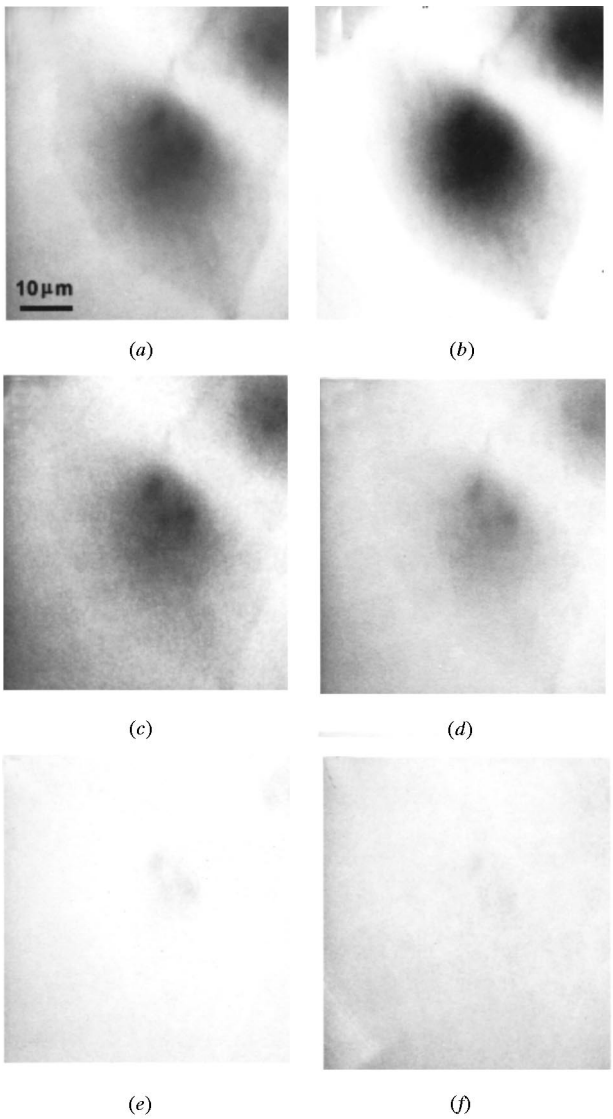

Figure 4
Elemental distribution in an HeLa cell obtained by the least-squares method. (*a*) Image at 3.45 nm, (*b*) carbon, (*c*) nitrogen, (*d*) oxygen, (*e*) calcium, (*f*) iron.

3.2. *Elemental imaging of an interphase HeLa cell*

Fig. 4 presents images of C, N, O, Ca and Fe. They were obtained from the images observed at wavelengths 1.76, 1.83, 2.16, 2.36, 2.79, 3.16, 3.45, 3.65, 3.98 and 4.48 nm, and calculated using the least-squares method. The dense distributions of C, N and O were observed in a nuclear region; the denser areas may correspond to nucleolus. Ca still seems to be observed in the nuclear region, but Fe had a largely faint image. Taking other elements into account and incorporating them into the calculation will improve the fidelity of the images.

In conclusion, the present system worked successfully in the imaging with an absorption peak of the XANES profile, and in the elucidation of elemental distributions achieved by the computer program using the least-squares method. Further improvements for resolution and sensitivities of the chemical analyses are in progress.

We thank Dr Yoshinori Kitajima and Dr Katsumi Kobayashi for their expertise in the set-up of our system at BL-11B and BL-12A at the Photon Factory, respectively, Mr Takashi Morisawa for helping with the elemental analysis, and Mr Michael C. Faudree for helping with the English. This work was performed under the approval of the Photon Factory Advisory Committee (Proposal Nos. 93-G319, 95-G283 and 95-G284), and partly supported by a Grant-in-Aid for Scientific Research (A) from the Ministry of Education, Science, Sports and Culture.

References

Ade, H. *et al.* (1992). *Science*, **258**, 972–975.
Buckley, C. J. (1995). *Rev. Sci. Instrum.* **66**, 1318–1321.
Buckley, C. J. *et al.* (1993). *Proc. SPIE*, **1741**, 363–372.
Buckley, C. J. *et al.* (1994). *X-ray Microscopy IV*, edited by V. V. Aristov & A. I. Erko, pp. 207–212. Moscow: Bogorodskii Pechatnik.
Buckley, C. J. *et al.* (1995). *Rev. Sci. Instrum.* **66**, 1322–1324.
Henke, B. L. *et al.* (1993). *Atomic Data Nucl. Data Tables*, **54**, 181–342.
Ito, A. *et al.* (1996). *J. Microsc.* **181**, 54–60.
Ito, A. *et al.* (1997). Photon Factory Activity Report 1996 #14, p. 261. Photon Factory, Tsukuba, Ibaraki 305, Japan.
Kenny, J. M. *et al.* (1985). *J. Microsc.* **138**, 321–328.
Shinohara, K. *et al.* (1994). *X-ray Microscopy IV*, edited by V. V. Aristov & A. I. Erko, pp. 264–267. Moscow: Bogorodskii Pechatnik.
Shinohara, K. *et al.* (1997). *X-ray Microscopy and Spectromicroscopy*, edited by J. Thieme *et al.* Heidelberg: Springer-Verlag.
Zhang, X. *et al.* (1994). *Nucl. Instrum. Methods Phys. Res. A*, **347**, 431–435.